The Experimental Study and Finite Element Simulation of Residual Stress in Welded Sections of Steel P91 Pipes with Multi-pass Welding

Davood Azadi, Nosratollah Solhjoei
Department of Mechanical Engineering,
Najafabad Branch, Islamic Azad University, Najafabad, Iran
E-mail: Davidfreedom65@yahoo.com, Solhjoei@yahoo.com

SayedAli Mousavi*
Department of Mechanical Engineering,
Najafabad Branch, Islamic Azad University, Najafabad, Iran
E-mail: sayedali_mousavi@yahoo.com
*Corresponding author

Received: 20 December 2015, Revised: 21 January 2016, Accepted: 28 February 2016

Abstract: All the producing and assembling processes exert residual stress on the pieces that may lead to structural failure. Therefore, calculating the residual stress in such structures has been common in recent years. In this article, distribution of temperature and residual stress resulting from arc welding in three-pass butt joint in P91 austenitic stainless steel pipes is calculated and estimated using the finite element method and experimental data. Simulating the welding process has been carried out three- dimensionally using Abaqus software. Distribution of the arc thermal flux has been identified based on the Goldak two-elliptical model using DFLUX subprogram in Abaqus software. The numerical method has been employed by doing thermoelastoplastic analysis and the technique of birth and death of the elements to model the welding passes and the melted elements. Then, using central hole drilling method, residual stress gradient of the thickness at distance 3mm from the welding line on the pipe is measured. Finally, the maximum percentage of error, through the results obtained from experimental measurements and finite element method, was reported 27% which is scientifically reasonable .The results show that the residual environmental stress in the internal surface of the pipe from the welding central line to 8.7mm varies with the gradient of 610MPa from 296MPa to -314MPa. Such a drastic stress distribution leads to genesising some cracks on the welded pipes.

Keywords: Arc welding, Central hole drilling method, Finite element method**,** Goldak heat source model, Residual stress.

Reference: Davood Azadi, Nosratollah Solhjoei and Sayedali Mousavi, "The Experimental Study and Finite Element Simulation of Residual Stress in Welded Sections of Steel P91 Pipes with Multi-pass Welding", Int J of Advanced Design and Manufacturing Technology, Vol. 9/No. 3, 2016, pp. 41–47.

Biographical notes: **D. Azadi** received his BSc in Mechanical Engineering from Iran University of Science and Technology in 2009. He is currently Master Student in Mechanical Engineering at the Department of Mechanical Engineering, Najafabad Branch, Islamic Azad University, Najafabad, Iran. **N. Solhjoei** received his PhD and MSc in Mechanical Engineering from Pierre and Marie Curie University (France) and BSc from Shiraz University. His current research focuses on Finite Element, Computational Mechanics, and manufacturing. **S. A. Mousavi** received his PhD in Mechatronics from Eastern Mediteirian University (Cyprus). His current research focuses on Industrial Automation and Bio-mechatronics.

1 INTRODUCTION

One of the common types of joining pipes in oil, gas, petrochemical and power plant industries is the circumferential butt welding which includes several passes. Due to concentration of great heat, generated from shielded metal arc welding, the areas around the welding line are affected by the thermal cyclic loads. During the welding process, the heat distribution inside the material directly influences the mechanical features, distortion and residual stress which are remained after cooling. The tensional residual stresses on each piece are added to the imposed loads and cause the failure cracks to appear and develop on each piece. The residual stresses are intangible in particular because they satisfy the balance equations and one cannot find any tangible sign of their existence. Therefore, it is necessary to find accurate information about the tension resulted from the welding process to improve the pipe performance, dimensions and increase welding parameters. As the abilities of the computers had increased, the techniques of problem solving related to thermal transfer updated, using the finite element method.

Analyzing the welds and numerical method pioneered in 1960 by Hibbit and Marcal [1], Friedman [2], Westby [3] and Masubushi [4]. In 1978, Andersson [5] studied the distribution of residual stress at high and low levels of a base plate near the welding line using the two-dimensional finite element method. He showed that phase transmutations have an important influence on the residual stresses during the cooling cycle. Marcal [6] provided a summary of experiences in the welding simulation. In 1972, Chihoski [7] found a theory that explained why the welds crack in certain conditions. He concluded that there is a severe biaxial compressive stress field near the weld pool. There may be a gap or crack in front of the compressive field and a tensional field or crack behind it. According to his theory, changing the method of welding, the compressive field can be controlled. In order to prove his theory, Chihoski developed the Moire' Fringing Technique to measure the displacements during edge and butt welding.

Brickstad et al. [8] could calculate the welding residual stresses in multi-passes joining of thick pipes using an axial symmetrical two-dimensional model and independent analysis. Yajiang [9] studied the distribution of residual stress in welding joining of high-strength steel plates and showed that the tension along the welding has a more influence on the crack than the tension in other two directions. In 2010, using the Quick Welder software, Dean Deng et al. [10] also generalized the finite element method to simulate the thermal welding field and distribution of residual stress in the tubular three-dimensional model with multi-pass welding. In the research, the features of residual stress distribution in stainless SUS304 pipe that has been induced by arc welding with Tungsten shielding gas, has been studied numerically. He showed that the results of numerical simulation for axial and circumferential residual stresses near the start and end of the welding areas have a steep gradient and are basically different from other areas. In 2012, they use numerical simulation and experimental methods for estimating of residual stress distribution using the multi-pass welding in a pipe welding with the average diameter and the dissimilar metals.

Kumar has delineated the effects of different thermo-metallurgical processes like heating, softening, cooling and solid state phase transformation (SSPT) on temporal evolution of the stress-field resulting from laser welding [17]. Columnar and equated microstructural zones have been numerically modelled in the weld region of the pipe by Yaghi. He shows that FE microstructural regions have been corroborated by columnar and equated zones that have been mapped out on a cross-sectional macro image of the weld [13]. Yaghi indicates the importance of including Solid-state phase transformation in the simulation of residual stresses during the welding of P91 steel as well as the significance of PWHT on stress relaxation [14]. Venkata using Norton creep law implemented PWHT and determined the residual stresses after relaxation. His model and the predictions were validated using neutron diffraction measurements on welded and post weld heat treated plate's relaxation [20]. Other researches were conducted on automated measurements system for instruments that identify the residual stresses cause fatigue in rotary systems [21].

The goal of this research is the numerical methodology in multi-passes welding of P91 steel pipes using the Goldak heat model. Here, shielded metal arc welding is used to weld. In section 2.1, the literature review of welding heat and investigating of heat affected distance is mentioned. The results of the model simulating are compared with the results of the practical experiment that is conducted using the central hole drilling method.

2 Requirements of welding process modeling

The interaction of heat source (arc, electron radiation or laser) with the welding pool is a complex physical phenomenon that has not yet been modelled completely. The pressure distribution from the arc source, the effects of surface tension of the drops of electrode, the buoyancy and viscosity powers of molten metal make the pool to distort and lead to significant disturbances. Due to the influence of the arc, the heat input is distributed effectively throughout a work piece. Thus, the most significant challenge, in simulating the welding process, is to define a heat source model that can predict the temperature field in the welding, accurately. Based on the observations of the molten area, it is suggested that the three-dimensional model of two-elliptical is more realistic and flexible than every other model that has been introduced for heat sources so far. According to this model, the fractions ff and fr of thermal deposition in front and back quarters of the model are necessary for fr + ff = 2.

Distribution of power intensity in the front quarter is determined by the equation (1) [11], and similarly,

distribution of power intensity inside the two-elliptical for the back quarter is determined by equation (2) [11]. For the three-dimensional model, the above volume flux is directly entered into the Abaqus software and is applied to the welding line using the subprogram DFLUX that is written in FORTRAN.

$$q(x,y,\xi,t)=\frac{6\sqrt{3}f_fQ}{abc_f\pi\sqrt{\pi}}e^{-3x^2/a^2}e^{-3y/b^2}e^{-3[z+\upsilon(\tau-t)]^2/c_f} \quad (1)$$

$$q(x,y,\xi,t)=\frac{6\sqrt{3}f_rQ}{abc_r\pi\sqrt{\pi}}e^{-3x^2/a^2}e^{-3y/b^2}e^{-3[z+\upsilon(\tau-t)]^2/cr} \quad (2)$$

where $Q = \eta VI/\upsilon$, and is the net energy rate, η is the arc efficiency for SMAW welding equal to 0.6 ,I symbol in equation is abbreviation (arc voltage),V symbol is abbreviation of amperage, υ is the welding speed and τ is the welding time. The constants a, b, c_f and c_r are variables that are υ determined by the size and form of the welding pool. These constants are obtained based on the welding pool. The welding simulation includes a set of time steps which each of them offer welding passes. Each pass includes a set of time developments.

The maximum allowable temperature changing in each development is set to be 40°C. In welding simulation, the birth and death technique is used to model the changes of fillers during a specific amount of time. In this method, all the elements including fillers, that are alive in the next stages of analyses, must be generated. In addition, multiplying degree of difficulty of filling elements and reduction factor (10^{-6}, for example) together deactivates the elements. Similarly, the weight, vibration, specific heat and other features of deactivated elements becomes zero. The weight and energy of deactivated elements are eliminated from the sum of the models. When the elements revive, they are not added to the model, but they are activated simply through returning the weight, strength, loads, etc. back to their initial value.

2.1. Numerical Simulation

The SMAW welding process is simulated through the finite element method using the Abaqus software. Due to the symmetry of the sample, half of the welded steel pipe (P91) was modelled. Fig. 1 shows the thermomechanical properties related to the temperature of the welded and the base steel. The welding has been modelled circumferentially with three passes.

The boundary conditions were considered to transfer the convection and radiation heat. In the simulated model, 17000 linear cubic eight-node elements were used. The number of used elements were determined based on the analyzing the sensitivity of the elements. Therefore, the maximum number of displacing the pipe during a welding process was studied. Fig. 2 shows that when the number of elements is equal to 17000, the maximum number of displacements does not change.

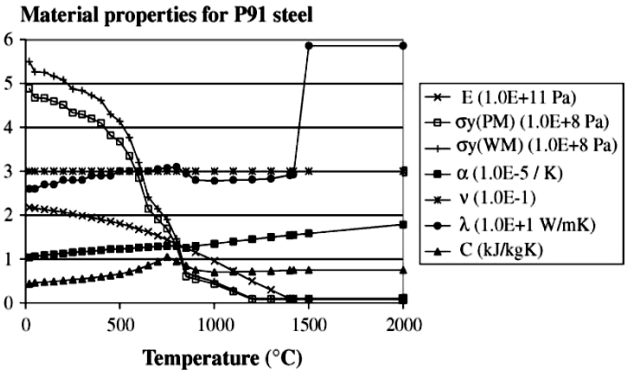

Fig. 1 The thermomechanical properties of the welded and base steel in terms of temperature used in analyzing the finite elements of P91 steel pipes [12].

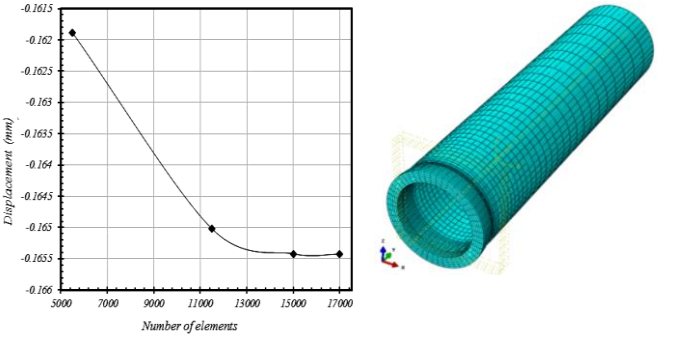

Fig. 2 The elements used in analyzing the finite element, 2B. The convergence of elements in simulating the welding process.

Table 1 The percentage of alloying elements resulting from the quantometer experiment for the P91 pipe samples

	Composition, %					
	N	Cb	Al	Ni	V	Mo
P91	0.05	0.1	0.3	0.35	0.2	0.85
	Cr	Si	S	P	Mn	C
P91	9	0.35	0.01	0.01	0.55	0.1

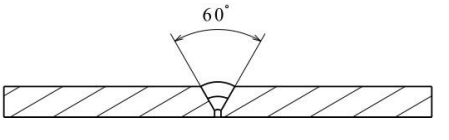

Fig. 3 Geometry and dimensions of the tested pipe

Table 2 The welding features for a 2-inch pipe

Speed (mm/s)	Amperage (A)	Voltage (V)	Bevel (Deg)	Number of passes
5-8	80-100	25-26	60	3

2.2. Experiments

The P91 steel pipes were circumferentially welded. In this method, two pipes with an outer diameter of 50.8, thickness of 6.35 and length of 250mm was used. In table 1, the quantometer results of the sample are represented that include the weight of the composition of chemical elements which are used. The pipes were welded without pre-heating in three passes. The order of welding layers on the pipe and the welding conditions are shown in Fig. 3 and Table 2.

2.2.1 An experiment for evaluating the residual stress

First, the imposed strain after drilling the central hole, is measured based on the groove depth. Then, using the strains created from the experiment and regarding to the equations of central hole drilling method, the residual stress of the piece is evaluated. In these experiments, the strainmeters of TML Co. (FRS-3-17) were used. In order to install the strainmeters, the surface of the work piece must be highly polished. Therefore, the installation location is polished with soft polishers (1000). This location must be exactly in the plate in front of the groove. In the sample, the strainmeter was installed in the part affected by the heat so that the center of strainmeter hole located in 3mm of the welding line.

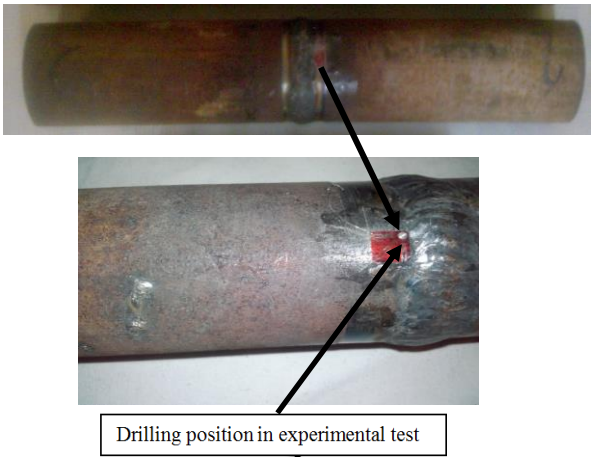

Fig. 4 The sample after the experimental test.

3 RESULTS

The thermal history of the welding process on the 2-inch pipe as shown in Fig. 5, in three points on the inner surface of the pipe at angles of 90, 180 and 270 and in similar distances from the central welding line is indicated in Fig. 6. The circumferential residual stresses in the inner and outer surfaces of the 2-inch pipe that are obtained from numerical simulation are represented in Figs.7 and 8. As it can be seen in Figs.7 and 8 stresses at the welding center (zero mm) are tensile. The more far from the center of welding, the tensile stress will be reduced and changed to the compressive stress. In the short distance from the welding line, in the heat affected zone, (about one centimeter) the maximum tensile stress changes to the maximum compressive stress, which shows that this area is the most probable one for cracking.

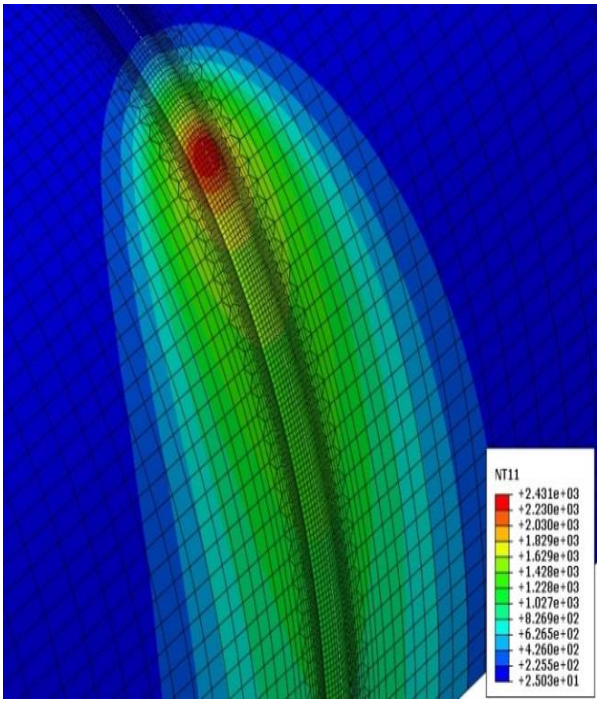

Fig. 5 The counters of temperature distribution of the molten pool 3-D model during welding.

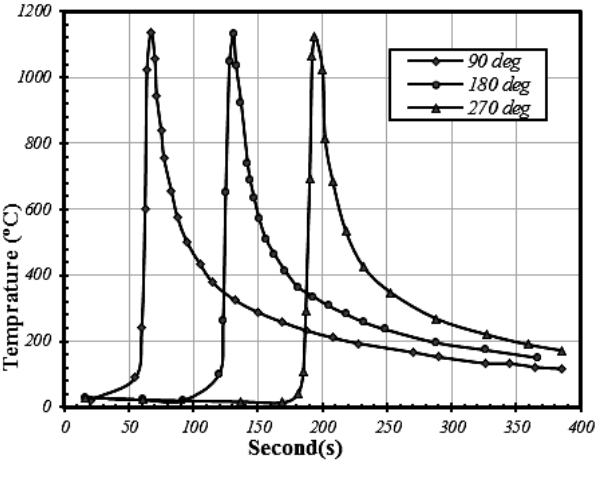

Fig. 6 The thermal history of welding on the 2-inch pipe.

In Fig. 9 the comparison of shear stress is shown. As shown, by comparing responses (residual stresses and displacements) the results show that samples with less displacement have less residual stresses and vice versa. In hoop welding the large axial tensile and compressive residual stress and radial deformations can be seen while in the distance far from the welding lines, large axial tensile

and compressive residual stresses are seen on the inner and outer plates.

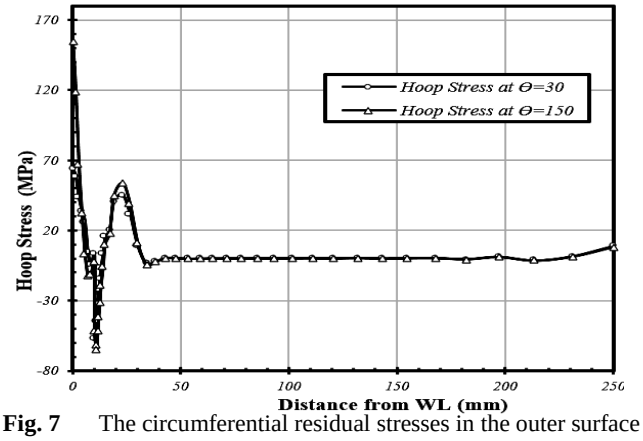

Fig. 7 The circumferential residual stresses in the outer surface of the pipe at the angles of 30 and 150 from the welding starting point.

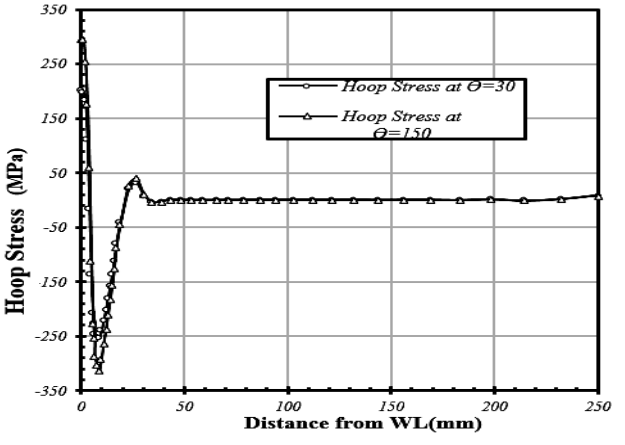

Fig. 8 The circumferential residual stresses in the inner surface of the pipe at the angles of 30 and 150 from the welding starting point

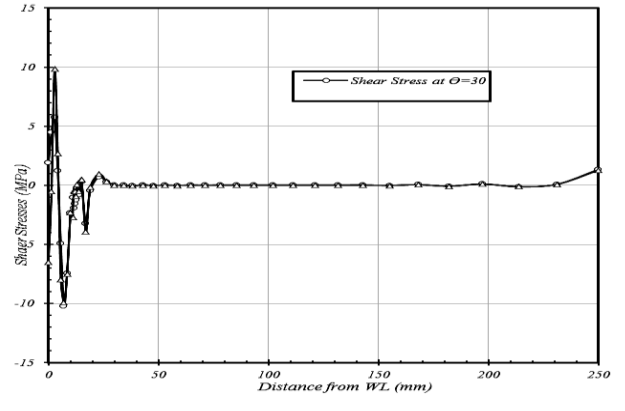

Fig. 9 The comparison of shear stress

In Fig. 10, the revealed strains after drilling in experimental test are indicated. It is worth mentioning that for evaluating the strains, the strainmeter is installed in 3mm from the welding line. It should be noted that the number of steps in drilling experiments is 35, depth of 2 mm .As it can be seen in Fig. 10, the axial strains are tensile while hoop strain in the first steps to the depth of 1.2mm is compressive and then in the depth to 2mm is tensile. The limitation of 2 mm is choosed according to the [19]. In Fig. 11, the stresses obtained from the finite element method and the experiments are compared.

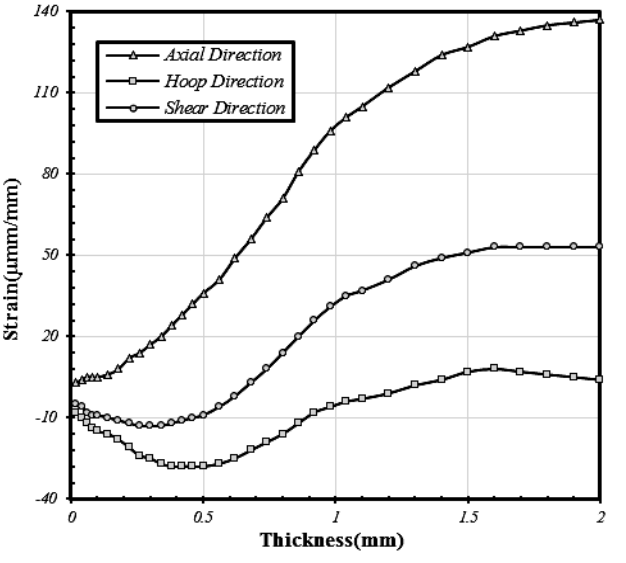

Fig. 10 2-inch pipe, the strains obtained from the experiment.

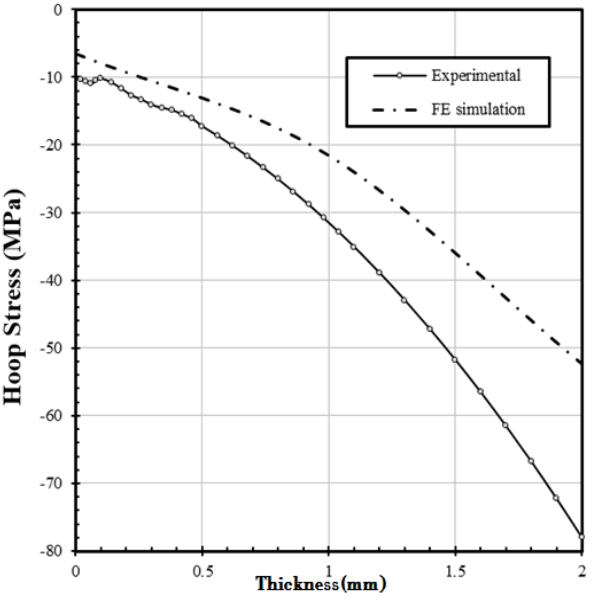

Fig. 11 2-inch pipe, the stresses obtained from the experiment and simulation.

3.1. Study of stress changes resulting from the pass welding

The residual stresses caused by welding in different passes are subjected to change. In this section, the changes will be discussed using numerical simulations. For this purpose, on

a pipe with the outside diameter, thickness and length of, respectively, 2, 1/4, 20 inches, three pass welding is simulated. The simulation results are brought in Fig. 12. These forms show the environmental and thrust stresses in the inner surface of the tube. As it is shown, the volume of the passes is increased and therefor the input energy, which is a function of welding volume, is increased .Then, it can be concluded that the level of induced residual stresses is increased.

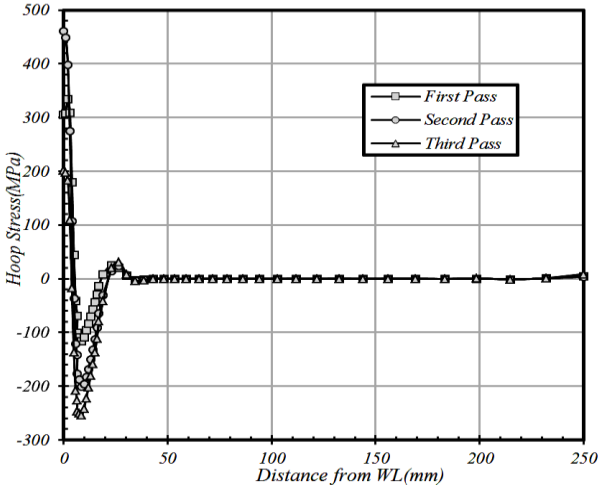

Fig. 12 Changes in environmental stresses on the inner surface of the tube along the length of the tube by increasing the number of passes

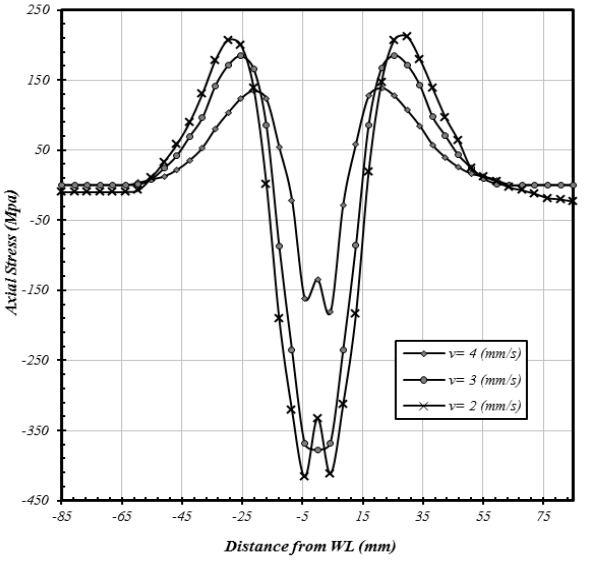

Fig. 13 Axial stress by changing the linear velocity changes

3.2. The effect of linear velocity on the surface of welding residual stress

The axial residual stress fields for welding linear speeds equal to 2, 3 and 4 (mm/s), which are used in the simulations , is shown in Fig. 13. Maximum tensile stresses at the least linear welding speed, i.e. 2 (mm/s), can be seen on the outer surface of the pipe. Similarly, the minimum tensile stress at the most linear welding speed, that is 4 (mm/s), can be seen on the outer surface of the pipe. The less welding speed, increases input heat per volume unit which causes the melting and heat-affected zone larger. So the level of the induced residual stresses increase.

3.3. The effect of the amperage changes on the level of residual stress

Fig.14 shows the axial tension in the outer surface of pipe for three different currents of 150, 200 and 300 amp, holding all other variables constant. Increasing of the amperage causes the overall input heat per volume unit increase. The effects of input heat per volume unit is directly on the temperature distribution and the resulting residual stress graph in welded structures , in the condition that the linear welding speed and all other variables are held constant.

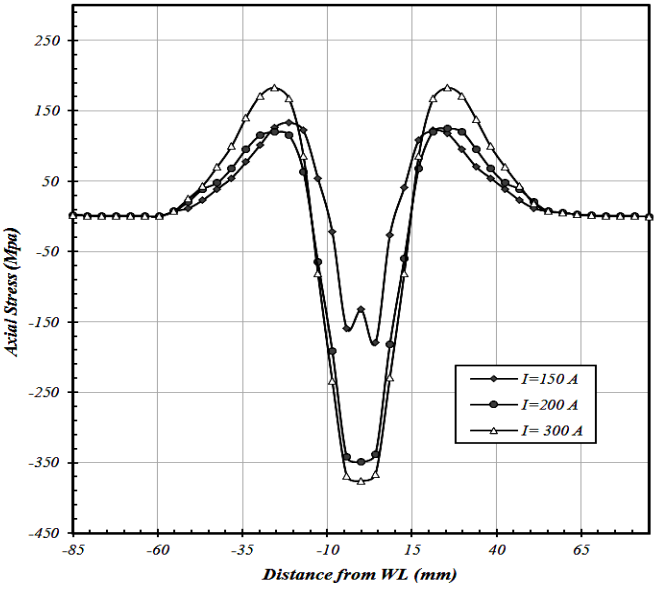

Fig. 14 Residual axial stress on the outer surface of the tube at 150 degrees from the starting point for the different welding brazing

4 CONCLUTION

In this article, the residual stresses in multi-pass welding that was done circumferentially on stainless steel pipes were studied. Comparing the results of numerical simulation with practical measurements, the acceptable accuracy of simulations is presented. The results of detailed study of environmental residual stresses in the welding part and the area affected by the heat are shown in Figs. 7 and 8 in which the stress gradient in 12mm from the welding line is very high. In addition, the results of analyzing the finite element show that the maximum tensile stresses and the

maximum compressive stresses are created in the central welding line and the area affected by the heat respectively.

As it is clear, the maximum tensile and compressive stresses are created in the inner surface of the pipe; therefore, this surface is susceptible of cracks resulted from welding residual stress. In all mechanical methods of measuring residual stresses, a part of material is removed or eliminated. Now regarding the fact that a part of material is removed, the stresses related to that area will be removed too, the former residual stress distribution that was tending to equilibrate will be changed. In other words, it does not remain in an equilibrated state any more. Thus, the object is transformed to achieve equilibrium and this transformation is registered in measurement methods. Then, using the relations given for the central drilling method, the residual stress of the piece will be calculated.

The problem confronting the mechanical methods or the methods that remove a part of material is the plasticity effect in the object. Until the object is in the elastic form, the piece will be returned to its original state by removing the external load. The transformations made in the object are not permanent, but as the object is transformed to plastic, the made transformations are not reversible anymore and remain in the object. Since the central hole drilling method is based on releasing the elastic stress, the plasticity during strain releasing process can lead to make error in measurement. On the other hand, due to the inherent and computational errors of the finite element method, there is a deviation between numerical solution and the practical method.

5 REFRENCES

[1] Hibbitt H. D., Marcal P. V., 1973, "A numerical thermo-mechanical model for the welding and subsequent loading of a fabricated structure", Company and Structure, Vol. 3, pp. 1145-1174.

[2] Friedman, E., 1978, "Analysis of weld puddle distortion", Welding J Research Suppl., pp. 161-166.

[3] Westby O., 1968, "Temperature distribution in the workpiece by welding", Department of Metallurgy and Metals Working, The Technical University, Trondheim Norway.

[4] Masubushi, K., 1980, "Analysis of welded structures", Pergamon Press, and Fracture mechanics applications in failure studies, Materials Characterization, Vol 33.

[5] Andersson B. A. B., 1978, "Thermal stresses in submerged-arc welded joint considering phase transformation", Journal of Engineering Materials and Technology, Trans. ASME, Vol. 100, pp. 356-362.

[6] Marcal P., 1974, "Structural mechanics programs", Charlottesville, University Press, pp. 191-206.

[7] Chihoski R. A., 1972, "Understanding weld cracking in Aluminum sheet", Welding Journal, Vol. 25, pp. 24-30.

[8] Brickstad, B. and Josefson, B. L., 1998, "A parametric study of residual stresses in multi-pass butt-welded stainless steel pipes", International Journal of Pressure Vessels and Piping, Vol. 75, pp. 11-25.

[9] Yajiang, L., Juan, W., Maoai, C. and Xiaoqin, S., 2004, "Finite element analysis of residual stress in the welded zone of a high strength steel", Bulletin of Materials Science, Vol. 27(2), pp. 127-132.

[10] Dean D., Shoichi K., 2010, "FEM prediction of welding residual stresses in a sus304 girth-welded pipe with emphasis on stress distribution near weld start/end location", Computational Materials Science, Vol. 50, pp. 612-621.

[11] Goldak, J., Chakravarti, A., Bibby, M., 1984, "A new finite element model for welding heat sources, Metallurgical Transactions", Vol 15B, PP 299-305.

[12] Yaghi, A., Hyde, T. H., Becker, A. A., Sun1, W., Williams, J. A., Pathiraj, B., 2005, "Simulation of residual stresses in welded p91 pipes", 5th International Conference on Mechanics and Materials in Design, Chapter IV, pp. 1-15.

[13] Yaghi. A., Hyde. T., Becker. A., Sun. W., 2009, "Thermo-mechanical modeling of weld microstructure and residual stresses in P91 pipes", Energy Material 4 (3), 113-123.

[14] Yaghi. A, Hyde. T., Becker. A., William. J., Sun. W., 2008. "Finite element simulation of welding and residual stresses in a P91 steel pipe incorporating solid state phase transformation and post weld heat treatment", Journal of Strain Analysis for Engineering Design, 43 (5), 275-293.

[15] Kim. S., Kim. J., Lee. W., 2009, "Numerical Prediction and neutron diffraction measurement of residual stress for modified 9Cr-1Mo steel", Journal of material Processing Technology, 167 (2), 480-487.

[16] Deng, D., Murakawat, H., 2006, "The Prediction of welding residual stress in multi-pass butt-welded modified 9Cr–1Mo steel pipe considering phase transformation effects", Computational Material science, 37 (3), 209-219.

[17] Kumar, S., Awasthi, R., Vishwanadham, C. S., Bhuanumurthy, K., Dey, G. K., 2014, "Thermo-metallurgical and thermo-mechanical computations for laser welded joint in 9Cr–1Mo (V, Nb) ferritic/martensitic steel", Materials and Design, 59, 211-220.

[18] Zubairuddin, M., Alber, S. K., Mahadevan, S., Vasudevan, M., Chaudhari, V., Suri, V. K., 2014, "Experimental and Finite element analysis of residual stress and distortion in GTA welding of modified 9Cr-1Mo steel", Journal of Mechanical Science and Technology, 28 (12), 5095-5105.

[19] Schajer, G. S., 1988, "Measurement of Non-uniform Residual Stresses Using the Hole- Drilling Method", Part II—Practical Application of the Integral Method, Journal of Engineering Materials and Technology, 110(1), 344-349.

[20] Abburi Venkataa, K., Kumarb, S., Deyc, H. C., Smitha, D. J., Bouchardd P. J., and Truman, C, E., 2014, "Study on the Effect of Post Weld Heat Treatment Parameters on the Relaxation of Welding Residual Stresses in Electron Beam Welded P91 Steel Plates", Procedia Engineering, l 86 (1) ,223–233.

[21] Jamshidian, M., Mousavi, S. A., 2015, "Thickness Measuring of Thin Metal by Non Destructive with Fuzzy Logic Control System", Journal of Modern Processes in Manufacturing and Production, Vol. 4(4), 39-45.